Optimal Interventions for Epidemic Outbreaks

Abstract of Ph.D. Thesis

Khalil Muqbel

Supervisor:

Prof. Dr. Gergely Röst

Doctoral School of Mathematics
and Computer Science
University of Szeged, Bolyai Institute

Szeged

2020.

Introduction

Switching models have been used recently in the compartmental models of mathematical epidemiology to analyze the impact of control measures on the disease dynamics. For example, it has been observed that if the treatment rate [10] or the incidence function [1] is non-smooth, that may lead to various bifurcations. These sharp changes occur in [1] and [10] when the total population, or the infected population reaches a threshold level. Such a sudden change may even be discontinuous, for example due to the implementation and termination of an intervention policy such as vaccination or school closures. Mathematically, such situations are described by Filippov systems, when the phase space is divided into two (or more) parts and the system is given by different vector fields in each of those parts. Examples include sudden changes in vaccination [6, 8], hospitalization [11], transmission [12], travel patterns [4], or the combination of several effects [9]. They have been used for vector borne diseases as well [13]. An overview of the basic theory and applications of switching epidemiological models can be found in [5]. Many of the mathematical challenges appear due to the incompatible behaviours of the vector fields at their interfaces, on the so-called switching manifold.

This thesis aims to propose a family of temporary intervention strategies. For the sake of simplicity, we work in the basic SIR-framework. An intervention strategy will be defined by two parameters which determine the time interval it is applied as well as the intensity of intervention. Our goal is to find out which strategy is the most cost-efficient, where costs are assigned to cases of infections and intervention. Furthermore, we construct a final size system for each strategy and investigate which strategy is better to minimize the final epidemic size. In addition we propose and analyze a mathematical model for infectious disease dynamics with a discontinuous control function, where the control is activated with some time delay after the density of the infected population reaches a threshold. Our results provide insight into disease management, by exploring the effect of the interplay of the control efficacy, the triggering threshold and the delay in implementation. This thesis is based on the following publications:

- Muqbel, K., Dénes, A. and Röst, G., 2019. Optimal Temporary Vaccination Strategies for Epidemic Outbreaks. *In Trends in Biomathematics: Mathematical Modeling for Health, Harvesting, and Population Dynamics*, pp. 299-307. Springer, Cham;
- Muqbel, K., Vas, G. Röst, G., 2020. Periodic Orbits and Global Stability for a Discontinuous SIR Model with Delayed Control. *Qual. Theory Dyn. Syst.* **19**, 59.

Optimal temporary vaccination strategies for epidemic outbreaks

We consider a constant population divided into susceptible ($S(t)$), infected ($I(t)$), and removed ($R(t)$) compartments. New infections occur with transmission coefficient β and infected individuals recover with rate α. Upon recovery, full immunity is assumed. Vaccination of susceptibles is included in the model with time dependent vaccination rate $v(t)$, to be specified later. Vaccination is assumed to be fully protective, thus vaccinated individuals are placed in the R-compartment as well. Hence, we consider the following system of differential equations:

$$\begin{aligned} S'(t) &= -\beta S(t)I(t) - v(t)S(t), \\ I'(t) &= \beta S(t)I(t) - \alpha I(t), \\ R'(t) &= \alpha I(t) + v(t)S(t), \end{aligned} \tag{1}$$

with the initial data $S(0) = S_0$, $I(0) = I_0$, $R(0) = 0$, where I_0 is relatively small compared to the total population size $N = S + I + R$. The basic reproduction number is given by $\mathcal{R}_0 = \beta S_0/\alpha$, however by normalizing the population size at $N = 1$ and with $I_0 << 1$, we have $S_0 \approx 1$ hence the reproduction number simplifies to $\mathcal{R}_0 = \beta/\alpha$. Epidemic outbreak occurs when $\mathcal{R}_0 > 1$.

The total cost (TC) of an outbreak will be assessed by considering two components, the disease burden and the cost of vaccination. Disease burden is calculated as the total number of infections during the course of the outbreak (denoted by $\tilde{I}$) multiplied by the cost C_1 of a single infection. Vaccination cost is calculated as the total number of administered vaccines (denoted by $\tilde{V}$) multiplied by the cost C_2 of a single vaccination. This way, for the total cost we have

$$TC \coloneqq C_1\tilde{I} + C_2\tilde{V}, \tag{2}$$

where

$$\tilde{I} \coloneqq \int_0^\infty \beta S(t)I(t)dt = \alpha \int_0^\infty I(t)dt, \tag{3}$$

$$\tilde{V} \coloneqq \int_0^\infty v(t)S(t)dt. \tag{4}$$

We call such an intervention a *VUHIA*-strategy of (k, p)-type, referring to *vaccinate until herd immunity achieved* with parameters (k, p).

In mathematical terms, the *VUHIA*-strategy of (k, p)-type is defined as follows. Let

$$v(t) = \begin{cases} 0, & t \notin J, \\ p, & t \in J, \end{cases}$$

where J is the intervention interval $J = [T_{\text{start}}, T_{\text{end}}]$ with

$$T_{\text{start}} = \min\{t \geq 0 : I(t) \geq k\} \tag{5}$$

and

$$T_{\text{end}} = \min\{t \geq 0 : \beta S(t) - \alpha \leq 0\}. \tag{6}$$

The time T_{start} is well defined as long as $k \in [I_0, I_{\max}]$, where $I_{\max}$ denotes the peak of the SIR-epidemic in the absence of any intervention. It is well known for the SIR model (with $N = 1$) that

$$I_{\max} = 1 - \mathcal{R}_0^{-1}(1 + \log \mathcal{R}_0). \tag{7}$$

Clearly we have $I'(t_*) = 0$ when $S(t_*) = \alpha/\beta$, and $I'(t) < 0$ for any $t > t_*$ regardless we vaccinate or not at some $t > t_*$. Since the epidemic eventually always dies out, T_{end} is well defined, and (4) becomes

$$\tilde{V} \coloneqq p \int_{T_{\text{start}}}^{T_{\text{end}}} S(t)dt. \tag{8}$$

The advantages of the *VUHIA*-strategy are the following. First, it has a clear and meaningful definition: we start vaccinate with rate p when a threshold k is reached in the level of infection, and we start the vaccination then the number of susceptibles drops below $\mathcal{R}_0^{-1}$, that is herd immunity achieved the number of infected will decrease anyway. Second, it is determined only by the parameters (k, p), hence all strategies from this family can be explored in a two dimensional parameter space.

We have assigned a total cost to each strategy composed of cost of disease burden and cost of vaccination, and systematically investigated the dependence of the total cost on the parameters. Essentially, we have found three types of behaviours:

(a) *vaccination cost is very low compared to the cost associated to disease burden*: in this case increasing the vaccination rate and start vaccination earlier reduce the total cost;

(b) *vaccination cost is very high compared to the cost associated to disease burden*: in this case the optimal strategy is to not vaccinate at all;

(c) *vaccination cost and disease burden cost are of similar magnitudes*: there may be non-monotone relationships between the vaccination rate, the starting threshold and the total cost.

These three typical behaviours are plotted into a heatmap in Figure 1. In case (c), it may happen that a better strategy is to start earlier but only if we can start sufficiently early, or, it better to increase vaccination rate but only if we can increase it to a sufficiently high level. If we cannot meet those criteria, then the best decision is to not vaccinate. The top plot of Figure 1 illustrates these intricate non-monotonicity properties.

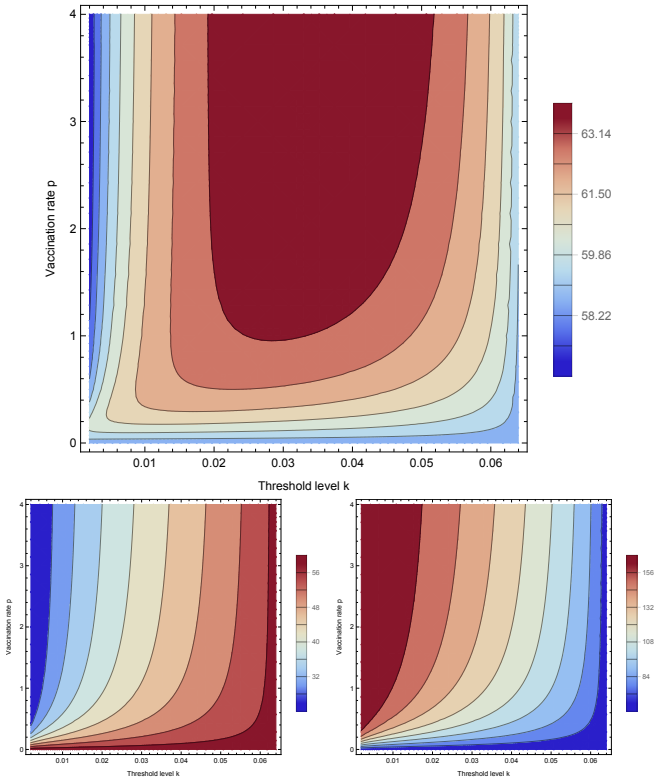

Figure 1: Dependence of the total cost on (k, p) in three typical situations: $C_2 = 50 \ll C_1$ (bottom left), $C_2 = 500 \gg C_1$ (bottom right), and $C_2 = 155$ (top). Parameters are $\mathcal{R}_0 = 1.5$, $\alpha = 6$, $\beta = 9$, and $C_2 = 50, 155, 500$ respectively. The bottom plots show monotone cases, while in the top plot we can find non-monotonicity in both k and p.

Optimal temporary non-pharmaceutical intervention strategies for epidemic outbreaks

In Chapter 4, we assume the following: At the beginning, an outbreak runs its natural course, hence new infections occur with transmission coefficient $\beta > 0$. However, if the number of infected individuals reaches a threshold level k, then the authorities impose certain non-pharmaceutical interventions (NPIs) with control intensity $u_* \in (0, 1)$, resulting in a reduction in the transmission coefficient. This reduction is included in the model with time dependent NPIs intensity rate $u(t)$, to be specified later. Infected individuals recovered with rate α. Upon recovery, full immunity is assumed. Hence we consider the following system of differential equations:

$$\begin{aligned} S'(t) &= -[1-u(t)]\beta S(t)I(t), \\ I'(t) &= [1-u(t)]\beta S(t)I(t) - \alpha I(t), \\ R'(t) &= \alpha I(t), \end{aligned} \tag{9}$$

with the initial data $S(0) = S_0$, $I(0) = I_0$, $R(0) = 0$, where

$$u(t) = \begin{cases} 0, & t \notin J, \\ u_*, & t \in J, \end{cases}$$

and $J = [T_{\text{start}}, T_{\text{end}}]$ is the intervention interval. We call such an intervention a *ITHIR*-strategy of (k, u_*)-type, referring to *intervene till herd immunity reached* with parameters (k, u_*). Let $\tilde{S}(k, u_*) := \lim_{t\to\infty} S(t)$ when (k, u_*) strategy applied. Clearly, if $\tilde{S}(k, u_*) < \alpha/\beta$, then the herd immunity is reached in the population, and hence T_{end} is well defined and the length of intervention is $\tilde{T} \coloneqq T_{\text{end}} - T_{\text{start}}$. Otherwise, herd immunity will never be reached before a vaccine is available, and hence $\tilde{T}$ is unbounded. The quadratic total cost (TC_{qq}) of an outbreak will be assessed as

$$TC_{qq} \quad \coloneqq \quad C_1\tilde{I}_q + C_2\tilde{T}u_*^2, \tag{10}$$

where

$$\tilde{I}_q \coloneqq \int_0^\infty I^2(t)dt. \tag{11}$$

In addition, we define several structures of the total cost function that are mixed of linear, quadratic, and exponential cost functions (see for example [3]). Overview of cost functions we use can be found in Chapter 4 of the thesis. We systematically investigated the dependence of the total cost on the parameters. We identified a parameter region where the herd immunity will never reached before a vaccine is available, in which case the intervention is not feasible as its cost exceeds any given bound. Considering the feasible region of limited costs, we found the following:

(A) *NPIs cost is very low compared to the cost associated to disease burden*: in this case the optimal strategy lies on the boundary between the two regions, which is again not feasible. In this case we impose a restriction: we maximized the possible length of intervention, and then we could find the optimal strategy with such restriction;

(B) *intervention cost and disease burden cost are of similar magnitudes*: there may be non-monotone relationships between the control intensity, the starting threshold and the total cost, and in this case we can determine which strategy gives the minimal total cost;

(C) *intervention cost is very high compared to the cost associated to disease burden*: in this case the minimal cost is attained without controlling at all.

These three typical behaviors are plotted into a heatmap in Figure 2. In case (A) (see Figure 2 bottom left), if, for example, we considered the maximized possible length

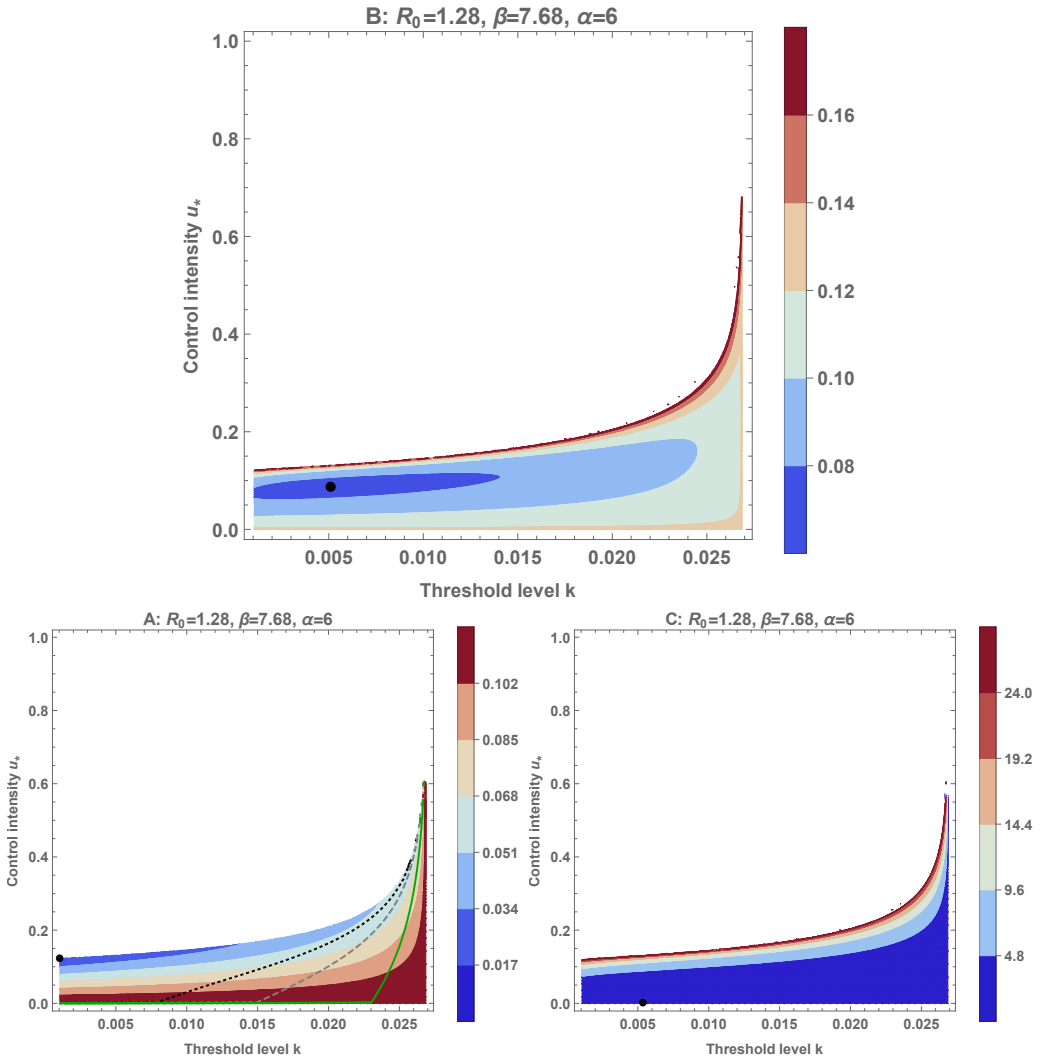

Figure 2: Dependence of the quadratic total cost on (k, u_*) in three typical situations: (A) $C_2 = 0.01 \ll C_1$, (C) $C_2 = 200 \gg C_1$, and (B) C_2 and C_1 are of similar magnitude. The white regions represent the unbounded total cost. The plots A and C show the monotone cases, while the plot B where $C_2 = 1$ we can find non-monotonicity in both k and u_*. In plot A the dotted black, dashed gray, and green curves represent the duration of NPIs for $1.5, 1, 0.5$ months respectively. The black point represents the infimum of the total cost in plot A, and it represents the minimum of the total cost in plot B and C.

of the intervention that represented by black dotted curve, which equals two months in this example, then the boundary between the two bounded and unbounded cost regions located outside this restricted domain, meaning that the optimal strategy lies in the feasible region which we could find it. If we maximized the possible control intensity to be in the feasible region, say that $0 < u_* < u_{\max}$ then the optimal strategy is to start the NPIs as early as possible with control intensity $u_* = u_{\max}$.

Furthermore, if we maximized both of the possible length of intervention and the possible control intensity, then their intersected point is the optimal strategy. In case (B), the black point in the Figure 2 (top) represents the global minimum of the quadratic total cost of seasonal flu when $C_2 = 1$, meaning that the optimal strategy is to start NPIs when $k = 0.005$ with control intensity $u_* = 0.088$. Depending on the available resources and public health capacities, there may be constraints on the parameters, such as $k_{\min} \leq k \leq I_{\max}$ and $u_* \leq u_{\max}$ in the feasible region. Finding the optimal strategy with such constraints can be found.

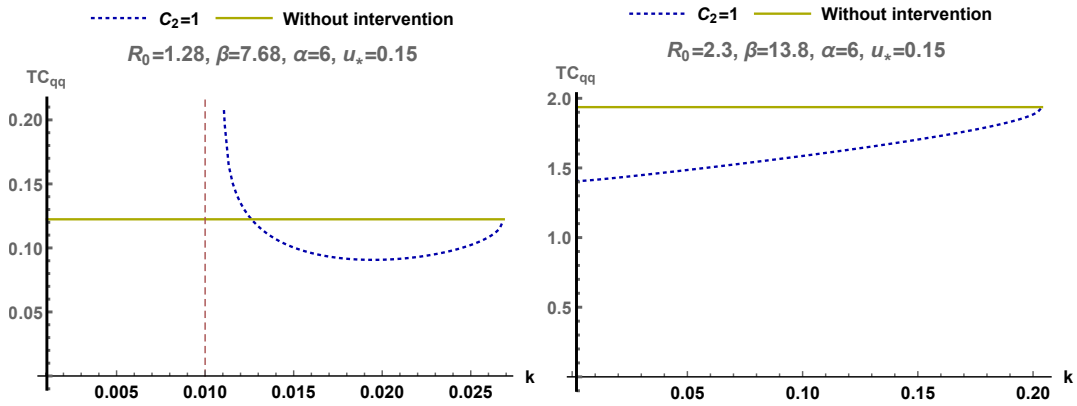

Figure 3: Effect of $\mathcal{R}_0$ on the monotonicity of the quadratic cost curve.

Another interesting phenomenon is depicted in Figure 3, showing that for a fixed u_*, the non-monotonicity of the total cost in k for seasonal influenza can be monotone increasing for COVID-19 and pandemic influenza. In that particular situation of Figure 3, for seasonal influenza, to minimize the cost we apply the strategy at the minimum while for pandemic influenza the lowest cost comes from start NPIs as early as possible. This important insight shows that pandemic influenza should be treated differently than seasonal influenza by public health authorities. Another interesting phenomenon is that for a fixed k, the monotonicity of the total cost in u_* can be reverse varying or nonmonotone depending on the cost function type.

Final epidemic size for temporary intervention strategies

The final epidemic size $(\tilde{I}(k,p))$ of *VUHIA*-strategy of (k,p)-type (with $N = 1$) is

$$\tilde{I}(k,p) := 1 - \tilde{S}(k,p) - \tilde{V}(k,p) = \int_0^\infty \beta S(t)I(t)dt = \alpha \int_0^\infty I(t)dt, \qquad (12)$$

where $\tilde{V}(k,p)$ is the total number of vaccinated individuals during the course of the epidemic and $\tilde{S}(k,p)$ is the total number of remained susceptibles after the epidemic dies out.

Theorem 1. *The final susceptible population size system for the VUHIA-strategy of (k,p)-type is*

$$\begin{aligned} k + S(T_{\text{start}}) - \mathcal{R}_0^{-1}\log S(T_{\text{start}}) &= 1 - \mathcal{R}_0^{-1}\log S_0, \\ k + S(T_{\text{start}}) - \mathcal{R}_0^{-1}\log S(T_{\text{start}}) + \frac{p}{\beta}\log k &= I(T_{\text{end}}) + \mathcal{R}_0^{-1} - \mathcal{R}_0^{-1}\log \mathcal{R}_0^{-1} + \frac{p}{\beta}\log I(T_{\text{end}}), \\ I(T_{\text{end}}) + \mathcal{R}_0^{-1} - \mathcal{R}_0^{-1}\log \mathcal{R}_0^{-1} &= \tilde{S}(k,p) - \mathcal{R}_0^{-1}\log \tilde{S}(k,p). \end{aligned} \tag{13}$$

Lemma 2. *Let $p > 0$ be a fixed vaccination rate. The final susceptible population size for VUHIA-strategy of (k,p)-type is decreasing in the threshold level k.*

Lemma 3. *Let $k \in [I_0, I_{\max}]$ be a fixed threshold level of starting vaccination. The final susceptible population size for VUHIA-strategy of (k,p)-type is increasing in the vaccination rate p.*

The final epidemic size of *ITHIR*-strategy of (k,u_*)-type (with $N=1$) is

$$\tilde{I}(k,u_*) := 1 - \tilde{S}(k,u_*) = \int_0^\infty (1-u_*)\beta S(t)I(t)dt = \alpha\int_0^\infty I(t)dt. \tag{14}$$

Theorem 4. *If $k \in [I_0, I_{\max}]$, then we distinguish two cases:*
Case 1: If $\tilde{S}(k,u_*) \geq \mathcal{R}_0^{-1}$, then the final size system for ITHIR-strategy of NPIs is

$$\begin{aligned} k + S(T_{\text{start}}) - \mathcal{R}_0^{-1}\log S(T_{\text{start}}) &= 1 - \mathcal{R}_0^{-1}\log S_0, \\ k + S(T_{\text{start}}) - \frac{\mathcal{R}_0^{-1}}{(1-u_*)}\log S(T_{\text{start}}) &= \tilde{S}(k,u_*) - \frac{\mathcal{R}_0^{-1}}{(1-u_*)}\log \tilde{S}(k,u_*). \end{aligned} \tag{15}$$

Case 2: If $\tilde{S}(k,u_*) < \mathcal{R}_0^{-1}$, then the final size system for ITHIR-strategy of NPIs is

$$\begin{aligned} k + S(T_{\text{start}}) - \mathcal{R}_0^{-1}\log S(T_{\text{start}}) &= 1 - \mathcal{R}_0^{-1}\log S_0, \\ k + S(T_{\text{start}}) - \frac{\mathcal{R}_0^{-1}}{(1-u_*)}\log S(T_{\text{start}}) &= I(T_{\text{end}}) + \mathcal{R}_0^{-1} - \frac{\mathcal{R}_0^{-1}}{(1-u_*)}\log \mathcal{R}_0^{-1}, \\ I(T_{\text{end}}) + \mathcal{R}_0^{-1} - \mathcal{R}_0^{-1}\log \mathcal{R}_0^{-1} &= \tilde{S}(k,u_*) - \mathcal{R}_0^{-1}\log \tilde{S}(k,u_*). \end{aligned} \tag{16}$$

Next we give a condition that determines whether we are in Case 1) or case 2) of the previous theorem.

Set

$$\eta(k) := 1 - \mathcal{R}_0^{-1}\frac{\log \frac{\mathcal{R}_0^{-1}}{S(T_{\text{start}})}}{\mathcal{R}_0^{-1} - k - S(T_{\text{start}})}. \tag{17}$$

Proposition 1. *Let $k \in [I_0, I_{\max}]$ be a given threshold level. If $\mathcal{R}_0^{-1} \leq \tilde{S}(k,u_*) < S(T_{\text{start}})$, then $\eta(k) \leq u_* \leq 1$.*

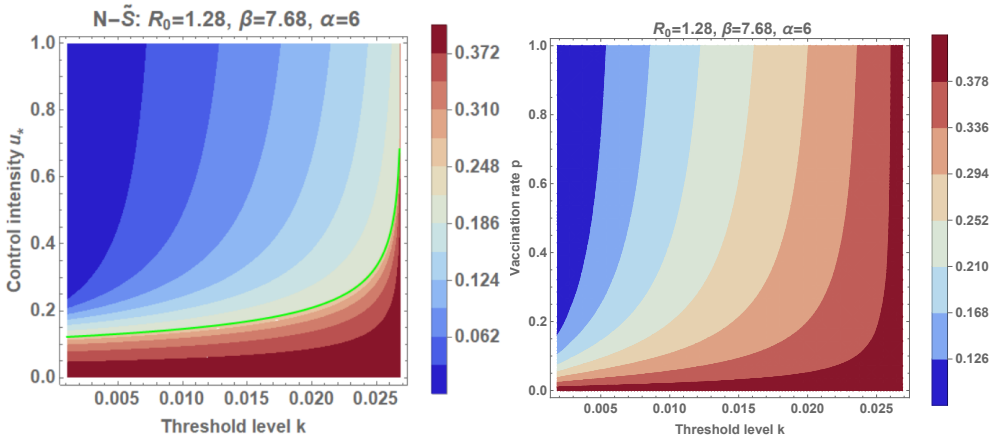

Figure 4: Dependence of the final epidemic size of NPIs on the control intensity u_* and on the threshold level k (left) and dependence of the final epidemic size of vaccination interventions on the vaccination rate p and on k (right). The green solid curve in the left plot represents the combination of $(k, u_* = \eta(k))$ that making the final epidemic size of NPIs equals the herd immunity threshold. That is $\tilde{I}(k, u_*) = 1 - \mathcal{R}_0^{-1} = 0.219531$ where $\tilde{S}(k, u_*) = \mathcal{R}_0^{-1}$. Herd immunity will never be reached in the region above the green curve. The final epidemic size without any intervention is $1 - S_\infty = 0.406805$.

In particular, if $k = I_0$, then $S(T_{\text{start}}) = S_0$ and the control intensity u_* in which $\tilde{S} = \mathcal{R}_0^{-1}$ is

$$u_* = 1 - \rho \frac{1}{1-\rho} \log \frac{S_0}{\rho}, \quad \text{where} \quad \rho = \frac{\alpha}{\beta} = \mathcal{R}_0^{-1}.$$

As a consequence of Proposition 1, $0 \le u_* < \eta(k)$ if $\tilde{S}(k, u_*) < \mathcal{R}_0^{-1}$.

Lemma 5. *Let $0 < u_* \le 1$ be a fixed control intensity. Then the final epidemic size $\tilde{I}(k, u_*)$ of ITHIR-strategy of NPIs is increasing in the threshold value k.*

Lemma 6. *Let $k \in [I_0, I_{\max}]$ be a fixed threshold level. Then the final epidemic size $\tilde{I}(k, u_*))$ of ITHIR-strategy of NPIs is decreasing in control intensity u_*.*

Figure 4 depicts the dependence of the final epidemic size of intervention strategies on the parameters where the plots are heatmaps. From this figure we can see that the FES is increasing in k while decreasing in u_* and decreasing in p. The minimal FES is attained by starting intervention as early as possible as high rate as possible. The green solid curve in the left plot represents the herd immunity threshold. The herd immunity will never be reached in the region above the green curve on contrast the other region below the green curve. Handel found that the best control strategy is the strategy that achieves this condition $(\tilde{S}, I_\infty) \to (\mathcal{R}_0^{-1}, 0)$ (see [2]). According to our finding w.r.t NPIs this occurs at the combination of (k, u_*) represented by the green solid curve and determined by the formula (17).

Periodic orbits and global stability for a discontinuous SIR model with delayed control

In Chapter 6 we consider the following SIR model with a delay $\tau > 0$:

$$\begin{aligned} \frac{dS(t)}{dt} &= \mu - \mu S(t) - [1 - u(I(t-\tau))]\beta S(t)I(t), \\ \frac{dI(t)}{dt} &= [1 - u(I(t-\tau))]\beta S(t)I(t) - \gamma I(t) - \mu I(t), \\ \frac{dR(t)}{dt} &= \gamma I(t) - \mu R(t), \end{aligned} \tag{18}$$

where

$$u(I) = \begin{cases} 0 & \text{if } I < k, \\ u_* & \text{if } I \geq k, \end{cases} \tag{19}$$

$k \in (0,1)$, $u_* \in (0,1)$, the reduction in transmission takes place with a time delay $\tau > 0$, $\gamma > 0$ is the recovery rate, and $\mu > 0$ is the birth and death rate.

In the special case $\tau = 0$ we obtain a model studied in [12].

Let (Sys_d) denote the system consisting of the first two equations of (18), (Sys_f) denotes the free system $(u(I) = 0)$, and (Sys_c) is for the control system $(u(I) = u_*)$.

As it is well-known, the set $\Delta = \{(S, I) \in [0,1]^2 : \quad S + I \leq 1\}$ is positively invariant for both (Sys_f) and (Sys_c). In other words, $\Delta_1 = \{(S, I) \in \Delta : I > 0\}$ is positively invariant w.r.t. both (Sys_f) and (Sys_c).

Because of the delay τ, the phase space for (Sys_d) has to be chosen as

$$X = \{(S_0, \varphi) \in [0,1] \times C([-\tau, 0], [0,1]) : S_0 + \varphi(0) \leq 1\}.$$

Consider the following subset of X:

$X_0 = \{(S_0, \varphi) \in X : [-\tau, 0] \ni t \mapsto \varphi(t) - k \in \mathbb{R}$ has a finite number of sign changes$\}$.

Chapter 6 only studies solutions with initial data in X_0. A further subset of X is

$$X_1 = \{(S_0, \varphi) \in X_0 : \varphi(0) > 0\},$$

the collection of endemic states, when the disease is present in the population.

In case of the free system (Sys_f), the basic reproduction number is $\mathcal{R}_0 = \beta/(\gamma + \mu)$. The reproduction number of the control system (Sys_c), what we call the control reproduction number, is given by $\mathcal{R}_{u_*} = (1 - u_*)\beta/(\gamma + \mu) = (1 - u_*)\mathcal{R}_0$.

The disease-free equilibrium for both (Sys_f) and (Sys_c) is

$$E_0^* = (S_0^*, I_0^*) \in \Delta, \qquad \text{where} \quad S_0^* = 1 \text{ and } I_0^* = 0.$$

The endemic equilibrium for (Sys_f) is

$$E_1^* = (S_1^*, I_1^*) \in \Delta, \qquad \text{where} \quad S_1^* = \frac{1}{\mathcal{R}_0} \text{ and } I_1^* = \frac{\mu}{\beta}(\mathcal{R}_0 - 1).$$

It exists only if $\mathcal{R}_0 > 1$. The endemic equilibrium for (Sys_c) is

$$E_2^* = (S_2^*, I_2^*) \in \Delta, \quad \text{where} \quad S_2^* = \frac{1}{\mathcal{R}_{u_*}} \text{ and } I_2^* = \frac{\mu}{(1-u_*)\beta}(\mathcal{R}_{u_*} - 1).$$

It exists for $\mathcal{R}_{u_*} > 1$. Proposition 2 examined what are the equilibria for (Sys_d).

Proposition 2.
The unique disease-free equilibrium for the delayed relay system (Sys_d) is $E_0^* \in X_0$, and it exists for all choices of parameters.
If $\mathcal{R}_0 \leq 1$, then there is no endemic equilibrium for (Sys_d). If $\mathcal{R}_0 > 1$, then we distinguish three cases.
(a) If

$$\mathcal{R}_0 > 1 \quad \textit{and} \quad \mathcal{R}_0[\mu - (\mu+\gamma)k] < \mu, \tag{C.1}$$

then $E_1^* \in X_0$ is the unique endemic equilibrium for (Sys_d).
(b) If

$$\mu \leq \mathcal{R}_0[\mu - (\mu+\gamma)k] < \mu/(1-u_*), \tag{C.2}$$

then there is no endemic equilibrium for (Sys_d).
(c) If

$$\mathcal{R}_0[\mu - (\mu+\gamma)k] \geq \mu/(1-u_*), \tag{C.3}$$

then $E_2^* \in X_0$ is the unique endemic equilibrium.

Note that if either (C.2) or (C.3) holds, then necessarily $\mathcal{R}_0 > 1$. In addition, conditions (C.1), (C.2) and (C.3) together cover the case $\mathcal{R}_0 > 1$.

In Fig. 5 we divide the (k, u_*) plane into three regions according to Cases (a)-(c) of Proposition 2 in order to show the interplay between threshold level k and control intensity u_*.

In Section 6.3 of the thesis we showed that if $(S_0, \varphi) \in X_0$ ($(S_0, \varphi) \in X_1$), then the solution (S, I) exists, and $(S(t), I_t) \in X_0$ ($(S(t), I_t) \in X_1$) for each $t \geq 0$.

Theorem 7. *If $\mathcal{R}_0 \leq 1$, then E_0^* is globally asymptotically stable for the delayed relay system (Sys_d) (that is, E_0^* is asymptotically stable and attracts X_0). If $\mathcal{R}_0 > 1$, then E_0^* is unstable w.r.t. (Sys_d), and the disease uniformly persists in the population.*

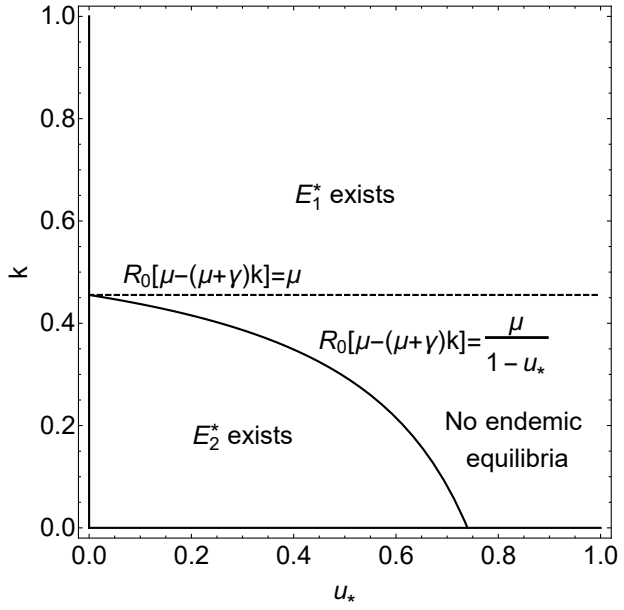

Figure 5: A 2-parameter bifurcation diagram giving the endemic equilibria in the (k, u_*) plane for $\mathcal{R}_0 > 1$. The parameters are $\gamma = 0.25$, $\beta = 2.5$ and $\mu = 0.4$.

Theorem 8. *If $\mathcal{R}_0 > 1$ and $k > k_0 = 1 - 1/\mathcal{R}_0$, then E_1^* is asymptotically stable with respect to (Sys_d), and it attracts the set X_1.*

Recall from Proposition 2 that (Sys_d) has no endemic equilibria if

$$\mu < \mathcal{R}_0[\mu - (\mu + \gamma)k] < \mu/(1 - u_*). \tag{20}$$

Theorem 9. *If (20) holds and τ is small enough, then the delayed relay system (Sys_d) has a periodic solution.*

Theorem 9 is the consequence of the Proposition 3. Now consider the subset

$$\mathcal{A} = \{(S_0, \varphi) \in X_1 : S_0 \in [S_1^*, 1 - k], \varphi(\theta) < k \text{ for } \theta \in [-\tau, 0) \text{ and } \varphi(0) = k\}.$$

Proposition 3. *If $(S_0, \varphi) \in \mathcal{A}$, then the solution $(S, I) = (S(.; S_0, \varphi), I(.; S_0, \varphi))$ of (Sys_d) is independent of φ. If (20) holds and τ is small enough, then there exists a smallest $t_1 = t_1(S_0) > 0$ such that $(S(t_1), I_{t_1}) \in \mathcal{A}$. Moreover, $S(t_1)$ depends continuously on S_0.*

Theorem 10. *Assume that*

$$\frac{\mu}{\mu + \gamma} + \frac{\mu}{\beta} < 2\sqrt{\frac{\mu}{\beta}} \tag{21}$$

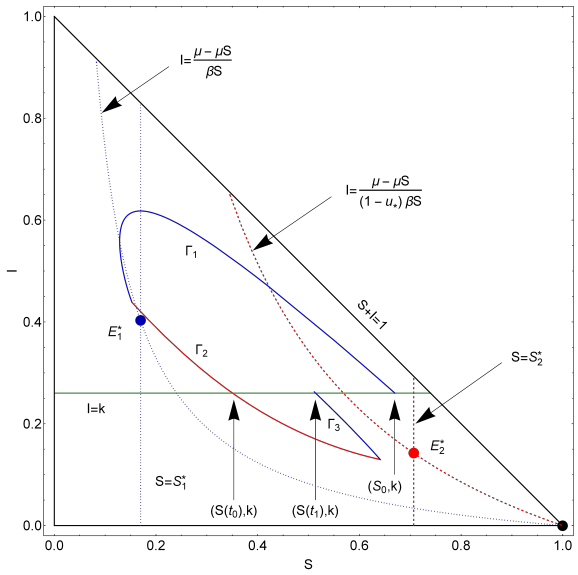

Figure 6: The solution $(S, I) = (S(.; S_0, \varphi), I(.; S_0, \varphi))$ of (Sys_d) for $(S_0, \varphi) \in \mathcal{A}$ under conditions (20) and $\mathcal{R}_{u_*} > 1$. The blue solid curves Γ_1 and Γ_3 represent (S, I) when it follows (Sys_f). The solid red curve Γ_2 represents (S, I) when it follows (Sys_c). The null-isoclines of (Sys_f) and (Sys_c) are the dotted blue and dashed red curves, respectively. The parameters are: $k = 0.26$, $\gamma = 1.38$, $\beta = 15.8$, $\mu = 1.3$, $\tau = 1$, $u_* = 0.76$, $S_0 = 0.58$.

and

$$k_1 = \frac{\mu}{\mu+\gamma} - S_2^* = \frac{\mu}{\mu+\gamma} - \frac{\mu+\gamma}{\beta(1-u_*)} > 0. \tag{22}$$

If $k \in (0, k_1)$, then E_2^* is the unique endemic equilibrium for (Sys_d), it is asymptotically stable, and the region of attraction is X_1.

Our results for (18)-(19) with delay $\tau > 0$ are summarized in Table 1. We have found that the behaviour of the system can be significantly different from switching models without delay. This can be easily seen by comparing Table 1 to Table 2, which lists the findings of [12] for system (18)-(19) in the case $\tau = 0$.

Fig. 7 depicts how the maxima and minima of some solutions (calculated after long time integration) change if parameter k increases. This numerically generated diagram confirms the conjecture that a periodic orbit may coexist with a stable equilibrium for some parameter configurations.

From our results we can draw some conclusions about the potential intervention strategies. For a large threshold k, the control will eventually be turned off and solutions converge to the endemic equilibrium of the free system, and the control strategy has no effect whatsoever. If $k < I_1^*$, then the control effort u_* also plays a role. If the control effort is weak, then $I_2^* > k$ (see Fig. 5) and we can expect the

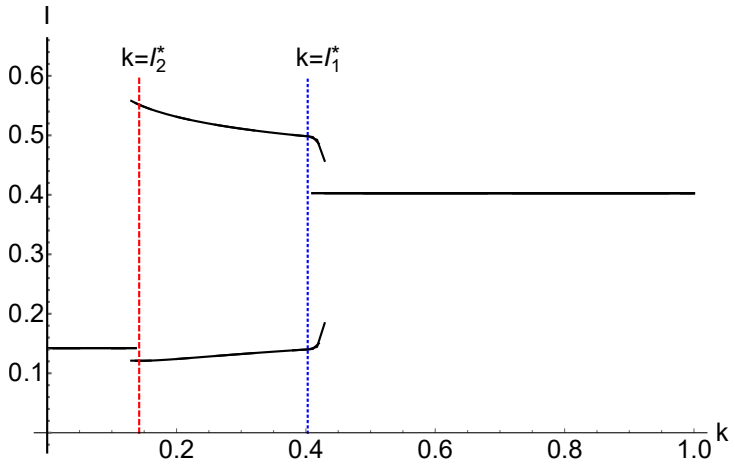

Figure 7: Plot of the maxima and minima of the I-terms after long time integration for several initial data. The bifurcation parameter is k. The other parameters are $u_* = 0.76$, $\gamma = 1.38$, $\beta = 15.8$, $\mu = 1.3$ and $\tau = 1$. The solution converges to E_2^* for small k, then to a periodic orbit as k increases, and then to E_1^* for large values of k.

control to be on for large times. Then the control strategy is reducing the infected population. Interestingly, in the presence of time delay, a strong control effort can induce periodic oscillations, and the peak of the periodic solution may be larger than the endemic level what we could achieve by a weaker control. If we do not want to tolerate high peaks in disease prevalence, we may choose a milder control strategy. Alternatively, we may try to reduce the delay as that leads to smaller oscillations, and then the periodic solution can be kept near the threshold k. Our results suggest that it may be worthwhile to continue research to the directions we initiated here, to have a better understanding of the effect of the interplay of control strategies and delays in implementation on the long term transmission dynamics.

	Parameters	Results for $\tau > 0$
	$\mathcal{R}_0 \leq 1$	E_0^* is GAS. No endemic equilibria.
(a)	$\mathcal{R}_0 > 1$ and $\mathcal{R}_0[\mu - (\mu+\gamma)k] < \mu$	E_0^* is unstable. E_1^* is the unique endemic equilibrium. E_1^* attracts X_1 for large k.
(b)	$\mu < \mathcal{R}_0[\mu - (\mu+\gamma)k] < \mu/(1-u_*)$	E_0^* is unstable. No endemic equilibria. Periodic solution for small τ.
(c)	$\mathcal{R}_0[\mu - (\mu+\gamma)k] > \mu/(1-u_*)$	E_0^* is unstable. E_2^* is the unique endemic equilibrium. E_2^* attracts X_1 for small k (under certain technical conditions).

Table 1: A summary of our results.

	Parameters	Results for $\tau = 0$
(a)	$\mathcal{R}_0 > 1$ and $\mathcal{R}_0[\mu - (\mu+\gamma)k] < \mu$	E_1^* is the unique endemic equilibrium, it attracts Δ_1.
(b)	$\mu < \mathcal{R}_0[\mu - (\mu+\gamma)k] < \mu/(1-u_*)$	A new equilibrium appears on the switching manifold attracting Δ_1.
(c)	$\mathcal{R}_0[\mu - (\mu+\gamma)k] > \mu/(1-u_*)$	E_2^* is the unique endemic equilibrium, it attracts Δ_1.

Table 2: The results of Xiao, Xu, and Tang in [12] for $\tau = 0$.

References

[1] Arino, J. and McCluskey, C.C., 2010. Effect of a sharp change of the incidence function on the dynamics of a simple disease. J. Biol. Dyn., **4**(5), pp.490-505.

[2] Handel A, Longini IM, Antia R., 2007. What is the best control strategy for multiple infectious disease outbreaks? Proceedings of the Royal Society B: Biological Sciences. 274(1611):833-837. doi:10.1098/rspb.2006.0015.

[3] Lin, F., Muthuraman, K., Lawley, M., 2010. An optimal control theory approach to non-pharmaceutical interventions. BMC infectious diseases 10(1), 32

[4] Liu, X. and Stechlinski, P., 2013. Transmission dynamics of a switched multi-city model with transport-related infections. Nonlinear Anal. Real World Appl., **14**(1), pp.264-279.

[5] Liu, X. and Stechlinski, P., 2017. Infectious disease modeling, a hybrid system approach, vol. 19. Springer.

[6] Muqbel, K., Dénes, A. and Röst, G., 2019. Optimal Temporary Vaccination Strategies for Epidemic Outbreaks. In Trends in Biomathematics: Mathematical Modeling for Health, Harvesting, and Population Dynamics, pp. 299-307. Springer, Cham.

[7] Muqbel, K., Vas, G. Röst, G., 2020. Periodic Orbits and Global Stability for a Discontinuous SIR Model with Delayed Control. *Qual. Theory Dyn. Syst.* **19**, 59 .

[8] Wang, A. and Xiao, Y., 2013. Sliding bifurcation and global dynamics of a Filippov epidemic model with vaccination. Int J. Bifurcat. Chaos., **23**(08), p.1350144.

[9] Wang, A., Xiao, Y. and Smith, R., 2019. Dynamics of a non-smooth epidemic model with three thresholds. Theor Biosci., pp.1-19.

[10] Wang, W., 2006. Backward bifurcation of an epidemic model with treatment. Math. Biosci. **201**(1-2), pp. 58–71.

[11] Wang, A., Xiao, Y. and Zhu, H., 2017. Dynamics of a Filippov epidemic model with limited hospital beds. Math. Biosci. Eng., **15**(3), p.739.

World Health Organization, 2019. Global Influenza Strategy 2019-2030.

[12] Xiao, Y., Xu, X., Tang, S., 2012. Sliding mode control of outbreaks of emerging infectious diseases. Bulletin of mathematical biology, 74(10), 2403-2422.

BioSystems **93**(3), 240–249.

Zhou, Y., Yang, K., Zhou, K., Liang, Y., 2014. Optimal vaccination policies for an SIR model with limited resources. Acta biotheoretica, 62(2), 171-181.

[13] Zhou, W., Xiao, Y. and Heffernan, J.M., 2019. A two-thresholds policy to interrupt transmission of West Nile Virus to birds. J. Theor. Biol., **463**, pp.22-46.